Table I. Properties of $H_{1-x}Ag_xUO_2PO_4$ Samples[a]

sample	$10^4X_{Ag^+}$[b]	10^3P_{HCN},[c] atm	$10^{-6}K_1$,[d] atm^{-1}
A	0.87	8.2	1.4
B	1.1	4.6	2.0
C	1.9	4.0	1.3
D	2.3	2.1	2.0
E	6.7	1.1	1.1
F	9.2	0.89	1.2

[a] Samples of the "doped" solids were prepared by intercalative ion-exchange reactions, described in ref 1. [b] The silver content of the doped solids, expressed as a mole fraction, was determined from PL properties after acid dissolution, as described in ref 11. [c] The partial pressure of HCN that produces the same relative amount of PL intensity in a $AgUO_2PO_4$ (AgUP) sample as observed in the doped sample, thereby providing an estimate of the residual Ag^+ content in the AgUP sample (see text). The values of P_{HCN} corresponding to the doped samples have been labeled in Figure 1. [d] The equilibrium constant for eq 1, calculated by using eq 2 and the corresponding values in the table.

a family of standards, $H_{1-x}Ag_xUO_2PO_4$, having known small concentrations of Ag^+.

The points labeled A-F in Figure 1 are samples of HUP that have been "doped" with Ag^+ [1,11] and then exposed to HCN gas. The relative increase in PL intensity in passing from $P_{HCN} = 0$ to the saturation value[12] of P_{HCN} serves to locate the point on the curve of Figure 1. An expression for K_1,[13] eq 2, is obtained for

$$K_1 = X_{H^+}(P_{HCN}X_{Ag^+})^{-1} \quad (2)$$

(11) The mole fraction of Ag^+ in the doped samples was determined by dissolving them in HNO_3, measuring their PL intensity and lifetime, and comparing these values to those of standards that fit Stern-Volmer quenching behavior. Quenching of UO_2^{2+} PL in solution by Ag^+ ions has been reported previously: see Marcantonatos, M. D. *J. Chem. Soc., Faraday Trans. 1* **1979**, *75*, 2252.

(12) The saturation value was the tank HCN concentration of $\sim 1.6 \times 10^{-2}$ atm; however, the PL intensity did not increase noticeably even when the system was exposed to pure HCN.

these standards from P_{HCN} and the H^+ and Ag^+ mole fractions; for our PL data, X_{H^+} can be approximated as unity. Substitution of the Figure 1 data into eq 2 yields a consistent value for K_1 of $\sim 1.5 \times 10^6$ atm^{-1}, as shown in Table I.

It is instructive to compare K_1 with solution data. Equation 1 can be obtained by adding eq 3 and 4, where the compounds

$$Ag^+(aq) + HCN(g) \rightleftharpoons H^+(aq) + AgCN(s) \quad (3)$$

$$AgUO_2PO_4(s) + H^+(aq) \rightleftharpoons HUO_2PO_4(s) + Ag^+(aq) \quad (4)$$

in eq 4 are $H_{1-x}Ag_xUO_2PO_4$ solid solutions. Reported values of K_{eq} for eq 3, K_3, range from 6.6×10^5 to 7.4×10^7 atm^{-1}.[14,15] We have measured K_{eq} for eq 4, K_4, to be ~ 0.3,[16] so that reasonable agreement is obtained between K_1 and K_3K_4.

In summary, the reaction of AgUP with HCN gas illustrates the ability of a lamellar solid to serve as a medium for a classical analytical titration and to act as a chemical sensor. The techniques described herein should permit a broad variety of aqueous acid-base/precipitation reactions to be mimicked in a lamellar matrix.

Acknowledgment. We thank Professors L. F. Dahl and A. Clearfield, Dr. G. Rosenthal, and S. Zuhoski for helpful discussions and ONR for financial support.

(13) We treat the solid as an ion-exchange host. See: Bard, A. J. *Chemical Equilibrium*; Harper & Row: New York, 1966; p 143.

(14) Rossini, F. D. "Selected Values of Chemical Thermodynamic Properties"; Circular 500; U.S. Government Printing Office: Washington, DC, 1952; pp 222, 229, 594.

(15) *CRC Handbook of Chemistry and Physics*, 65th ed.; Weast, R. C., Ed.; CRC Press: Boca Raton, FL, 1984; p D-51.

(16) After samples of HUP had come to equilibrium with aqueous $AgNO_3$ solutions, the concentration of Ag^+ remaining in solution was measured with a Ag ion electrode.

(17) To whom correspondence should be addressed.

Department of Chemistry
University of Wisconsin—Madison
Madison, Wisconsin 53706

Gunther H. Dieckmann
Arthur B. Ellis*[17]

Received August 21, 1987

Articles

Contribution from the Departments of Chemistry, Faculty of Education, Mie University, Tsu, Mie 514, Japan, and Nara University of Education, Takabatake-cho, Nara, Japan

Binuclear Complexes of Ruthenium and Osmium Bridged by 2,2′-Bibenzimidazolate: Preparation, Electrochemistry, and Formation of Mixed-Valence Complexes

Masa-aki Haga,*[1] Takeko Matsumura-Inoue,[2] and Shinichi Yamabe[2]

Received December 16, 1986

The preparation and spectroscopic and electrochemical properties of new 2,2′-bibenzimidazolate- (BiBzIm-) bridged binuclear complexes of the general formula $[(bpy)_2M(BiBzIm)M'(bpy)_2]^{n+}$ (M = Ru, Os; M′ = Ru, Os, Co, Ni) are reported. The Os(II)-Os(III) mixed-valence complex shows multiple intervalence-transfer (IT) absorption bands at 4800 and 8180 cm^{-1} in the near-infrared region, which can be attributed to the orbital splitting of optically prepared Os(III) site by tetragonal distortion and spin-orbit coupling. The Ru(II)-Os(III) and Ru(II)-Ru(III) mixed-valence complexes also exhibit multiple IT bands. The bandwidths at half-intensity for IT bands are narrower than those expected from Hush's theoretical treatment. These new mixed-valence complexes belong to Robin and Day's class II. The comproportionation constant K_{com} for the complex M = M′ = Ru greater than that for the complex M = M′ = Os is observed. This result, contrary to the trends reported so far, is discussed in terms of the orbital mixing between metal sites and BiBzIm. The anionic BiBzIm bridging ligand can cause stabilization of the mixed-valence complex by reducing the positive charge on the complex. The comparison of a BiBzIm-bridged complex with a bpm-bridged one is also discussed in terms of the donor-acceptor property of the ligand.

Introduction

Binuclear transition-metal complexes have received much attention in recent years. Many types of binuclear complexes with bridging ligand have been synthesized and utilized in the studies of electron-transfer processes and metal-metal interactions.[3] The

(1) Mie University.
(2) Nara University of Education.

(3) (a) Creutz, C. *Prog. Inorg. Chem.* **1983**, *30*, 1. (b) Meyer, T. J. *Acc. Chem. Res.* **1978**, *11*, 94. (c) Taube, H. *Ann. N.Y. Acad. Sci.* **1978**, *313*, 481. (d) Geiger, W. E.; Connelly, N. G. *Adv. Organomet. Chem.* **1985**, *23*, 87.

0020-1669/87/1326-4148$01.50/0

Chart I

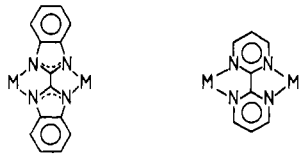

2,2'-Bibenzimidazolate (BiBzIm) 2,2'-Bipyrimidine (bpm)

selection of bridging ligand can change the nature of metal–metal interactions.[3a] Imidazolate, the conjugate base of imidazole, is known to act as a bridging ligand.[4] The presence of an imidazolate-bridged Cu(II)–Zn(II) binuclear center in bovine erythrocyte superoxide dismutase (SOD) has inspired the preparative studies of new discrete binuclear imidazolate-bridged transition-metal complexes.[5] The synthesis and electron-transfer kinetic studies of the complexes *trans*-$[(SO_4)(NH_3)_4Ru(Im)Co(NH_3)_5](BF_4)_3$ and $[(NC)_5Fe(Im)Co(NH_3)_5]^-$ (Im = imidazolate) have been reported.[6] The intramolecular electron-transfer rates are faster than those in analogous binuclear complexes with other bridging N-heterocycle ligands such as pyrazine. This suggests that imidazolate is particularly efficient in promoting electron transfer. Also, the mixed-valence Ru(II)–Ru(III) complex bridged by imidazolate has been reported. However, the complex was not stable.[6a] On the other hand, 2,2'-bibenzimidazolate (BiBzIm) can act as a symmetrical two-bidentate bridging ligand and is expected to stabilize binuclear complexes by the chelate effect. A similar bidentate bridging ligand, 2,2'-bipyrimidine (bpm), has also been used.[7] These two ligands (Chart I) give rise to almost the same metal–metal separation distance; however, the charge on the ligand is quite different, as BiBzIm is a dinegative ligand and bpm is neutral. Thus, these two ligands would afford different metal–metal interactions. The mixed-valence $[(bpy)_2Ru(bpm)Ru(bpy)_2]^{5+}$ complex (bpy = 2,2'-bipyridine) has been reported to be unstable.[7b] Recently, we reported the synthesis and electrochemical properties of binuclear Ru complexes bridged by BiBzIm and found that the mixed-valence $[(bpy)_2Ru(BiBzIm)Ru(bpy)_2]^{3+}$ was stable and exhibited multiple intervalence-transfer (IT) bands at 5130 and 9420 cm^{-1}.[8]

In this work, a systematic study of the synthesis, electrochemical, and spectral properties (UV and near-IR) of the new binuclear metal complexes bridged with BiBzIm, $[(bpy)_2M(BiBzIm)M'(bpy)_2]^{n+}$ (n = 2, 3, 4; M = Ru, Os; M' = Ru, Os, Co, Ni), is made, and the characteristics of their mixed-valence complexes are discussed on the basis of the IT band in near-IR region and an ab initio molecular orbital calculation for the ligand.

Experimental Section

Materials. The starting complexes $M(bpy)_2Cl_2$ (M = Ru, Os) were prepared by literature methods.[9,10] $[M(bpy)_2(BiBzImH_2)](ClO_4)_2$(M = Ru, Os; $BiBzImH_2$ = 2,2'-bibenzimidazole) were synthesized as reported earlier.[11,12] Tetrabutylammonium perchlorate (TBAP) was synthesized by the literature method,[13] recrystallized from ethanol three times, and vacuum dried at 70 °C. Acetonitrile was dried over phosphorus pentoxide, for spectral measurements, and further dried over calcium hydride before use for electrochemical measurements. All other chemicals were reagent grade and were used without further purification.

Preparations of Complexes. $[Os(bpy)_2(BiBzIm)]\cdot 4H_2O$. A methanol (50 cm^3) solution of $[Os(bpy)_2(BiBzImH_2)](ClO_4)_2\cdot 3H_2O$ (0.8 g, 0.81 mmol) was added to a sodium methoxide solution made up by the dissolution of sodium metals (0.07 g, 3.0 mmol) in methanol (20 cm^3). The solution immediately changed in color from yellow-brown to violet. After being refluxed for 1 h, the solution was then cooled to 0–5 °C in an ice bath. The resulting black microcrystalline solid was filtered, washed with a small amount of methanol, and dried in vacuo; 90% yield.

Anal. Calcd for $C_{34}H_{24}N_8Os\cdot 4H_2O$: C, 50.61; H, 3.99; N, 13.89. Found: C, 50.76; H, 3.12; N, 13.81.

$[(bpy)_2Os(BiBzIm)Os(bpy)_2](ClO_4)_2\cdot H_2O$. $Os(bpy)_2Cl_2$ (0.15 g, 0.26 mmol) was dissolved in ethanol/water (1:1 v/v, 50 cm^3) by refluxing the mixture for 0.5 h under nitrogen. $Os(bpy)_2(BiBzIm)\cdot 4H_2O$ (0.20 g, 0.25 mmol) and 30 cm^3 of ethanol/water (1:1 v/v) were added to the solution. The mixture was further heated and refluxed for 40 h; during this time the solid gradually dissolved, producing a dark brown solution. The solution was cooled to room temperature and filtered. To the filtrate an aqueous solution of sodium perchlorate (0.50 g, 3.6 mmol in 5 cm^3 H_2O) was added. The black precipitate was isolated by filtration and recrystallized from acetonitrile/ether; 56% yield.

Anal. Calcd for $C_{54}H_{40}N_{12}O_8Cl_2Os_2\cdot H_2O$: C, 44.60; H, 2.91; N, 11.56. Found: C, 44.40; H, 2.80; N, 11.56.

$[(bpy)_2Os(BiBzIm)Ru(bpy)_2](ClO_4)_2\cdot H_2O$. $Ru(bpy)_2Cl_2$ (0.16 g, 0.33 mmol) was suspended in methanol (40 cm^3) under nitrogen, and $Os(bpy)_2(BiBzIm)\cdot 4H_2O$ (0.25 g, 0.34 mmol) was added. The mixture was refluxed for 4 h, cooled to room temperature, and then filtered. An excess of sodium perchlorate (0.80 g, 5.7 mmol) was added to the filtrate to give a precipitate, which was collected and recrystallized from acetonitrile/ether; 60% yield.

Anal. Calcd for $C_{54}H_{40}N_{12}Cl_2O_8RuOs\cdot H_2O$: C, 47.51; H, 3.10; N, 12.31. Found: C, 47.20; H, 2.95; N, 12.36.

$[(bpy)_2Ru(BiBzIm)Co(bpy)_2](ClO_4)_2\cdot 2H_2O$. $Ru(bpy)_2(BiBzIm)\cdot 2H_2O$ (0.25 g, 0.37 mmol) was suspended in methanol/acetonitrile (14:1 v/v, 70 cm^3) and heated for 1 h with vigorous stirring. A mixture of cobalt(II) chloride hexahydrate (0.089 g, 0.37 mmol) and bpy (0.12 g, 0.77 mmol) in methanol (10 cm^3) was added. The resulting solution was refluxed for 0.5 h. During the course of reaction the solution changed in color from violet to red brown. After addition of 5 cm^3 of a saturated sodium perchlorate solution, the mixture was cooled and the brown red precipitate collected, washed with cold methanol, and dried in vacuo; 80% yield. μ_{eff} = 4.92 μ_B (25 °C).

Anal. Calcd for $C_{54}H_{40}N_{12}O_8Cl_2CoRu\cdot 2H_2O$: C, 51.80; H, 3.55; N, 13.43. Found: C, 51.86; H, 3.29; N, 13.59.

$[(bpy)_2Ru(BiBzIm)Ni(bpy)_2](ClO_4)_2$. A suspension of $Ru(bpy)_2(BiBzIm)\cdot 2H_2O$ (0.30 g, 0.4 mmol) in methanol (60 cm^3) was refluxed under nitrogen until dissolution was complete (ca. 0.5 h). To this violet solution was added nickel(II) acetate tetrahydrate (0.11 g, 0.4 mmol) in methanol (10 cm^3) and then bpy (0.14 g, 0.9 mmol). The solution was heated at reflux for 1 h, during which time the solution turned red brown. The reaction mixture was cooled and the product was precipitated from the solution by the addition of a saturated sodium perchlorate methanol solution (5 cm^3) and isolated by filtration; 73% yield. μ_{eff} = 3.24 μ_B (25 °C).

Anal. Calcd for $C_{54}H_{40}N_{12}O_8Cl_2NiRu$: C, 53.35; H, 3.32; N, 13.83. Found: C, 52.96; H, 2.72; N, 14.18.

Physical Measurements. Electronic spectra were obtained on a Shimadzu UV-210A double-beam spectrophotometer from 200 to 850 nm and a Hitachi 340 spectrophotometer from 800 to 2600 nm. For the measurements in the near-infrared region, a careful calibration of the base line was carried out. Infrared spectra were recorded by a Shimadzu IR-420 grating infrared spectrophotometer as Nujol mulls (4000–400 cm^{-1}). The magnetic susceptibility was determined by the Gouy method at room temperature (25 °C).

Cyclic voltammetric experiments were made with a Hokuto Denko HA 301 potentiostat with a Hokuto Denko HF-201 function generator and a Yokogawa 3086 A4 X-Y recorder. A three-electrode cell consisting of a Beckman stationary platinum disk, a platinum-flag counter electrode, and a saturated calomel reference electrode (SCE) was used. The reference electrode was separated from the cell by a salt bridge. The potentials were calibrated with respect to an internal ferrocene–ferrocenium (Fc/Fc^+) couple.[14]

Controlled-potential electrolysis experiments were performed at a large platinum-plate working electrode, with a Hokuto Denko HA-301 potentiostat and a Hokuto Denko HF-201 coulomb/amperohour meter. The reference electrode was the same SCE electrode used in the volt-

(4) Sundberg, R. J.; Martin, R. B. *Chem. Rev.* **1974**, *74*, 471.
(5) (a) Richardson, J. S.; Thomas, K. A.; Rubin, B. H.; Richardson, D. C. *Proc. Natl. Acad. Sci. U.S.A.* **1975**, *72*, 1349. (b) Strothkamp, K. G.; Lippard, S. J. *Acc. Chem. Res.* **1982**, *15*, 318.
(6) (a) Isied, S. S.; Kuehn, C. G. *J. Am. Chem. Soc.* **1978**, *100*, 6754. (b) Gulka, R.; Isied, S. S. *Inorg. Chem.* **1980**, *19*, 2342. (c) Szecsy, A. P.; Haim, A. J. *J. Am. Chem. Soc.* **1981**, *103*, 1679.
(7) (a) Hunziker, M.; Ludi, A. *J. Am. Chem. Soc.* **1977**, *99*, 7370. (b) Goldsby, K. A.; Meyer, T. J. *Inorg. Chem.* **1984**, *23*, 3002. (c) Ernst, S.; Kaim, W. *J. Am. Chem. Soc.* **1986**, *108*, 3578. (d) Kaim, W.; Kohlmann, S. *Inorg. Chem.* **1987**, *26*, 68.
(8) Haga, M. *Inorg. Chim. Acta* **1980**, *45*, L183.
(9) Sprintschnik, G.; Sprintschnik, H. W.; Whitten, D. G. *J. Am. Chem. Soc.* **1976**, *98*, 2337.
(10) Buckingham, D. A.; Dwyer, F. P.; Goodwin, H. A.; Sargenson, A. M. *Aust. J. Chem.* **1964**, *17*, 325.
(11) Haga, M. *Inorg. Chim. Acta* **1983**, *75*, 29.
(12) Bond, A. M.; Haga, M. *Inorg. Chem.* **1986**, *25*, 4507.
(13) Saji, T.; Yamada, T.; Aoyagui, S. *J. Electroanal. Chem. Interfacial Electrochem.* **1975**, *61*, 147.
(14) Gagne, R. R.; Koval, C. A.; Lisensky, G. C. *Inorg. Chem.* **1980**, *19*, 2854.

Table I. UV-Visible Absorption Spectral Data for $[(bpy)_2M(BiBzIm)M'(bpy)_2](ClO_4)_2$ in CH_3CN

M-M'	λ_{max}, nm (ϵ, M^{-1} cm^{-1})						
	$\pi-\pi^*$(bpy)[a]		$\pi-\pi^*$(BiBzIm)[b]		$d\pi-\pi^*$(bpy)		
Ru-Ru	245 (70 700)	294 (84 600)	318 (24 500)	355 (25 100)	505 (17 700)		
Ru-Os	244 (68 600)	293 (83 200)		357 (22 800)	501 (17 600)	683 (2380)	740 (2420)
Ru-Co	242 (69 000)	294 (77 600)	335 (28 400)		512 (10 400)		
Ru-Ni	243 (67 300)	294 (74 400)	337 (26 900)		513 (12 800)		
Os-Os	244 (61 900)	292 (82 600)		362 (20 000)	518 (18 250)	679 (4360)	732 (4380)

[a] The absorption band at 240 nm is comprised of both $\pi-\pi^*$(bpy) and $\pi-\pi^*$(BiBzIm) transitions. [b] The original $BiBzImH_2$ has absorption maxima at 315, 325, and 340 nm in ethanol.[39]

ammetric experiments and the auxiliary electrode was platinum gauze separated from the test solution by a salt bridge containing the solvent.

The spectroelectrochemistry was performed by using a platinum minigrid (80 mesh) working electrode in the cell designed originally by Lexa et al.[15] The cell was located directly in the spectrophotometer, and the absorption change was monitored during the electrolysis.

The Gaussian 80 program is used for the ab initio molecular orbital calculation of bridging ligands bpm and BiBzIm with the STO-3G basis set.[16] The geometry of bpm is generated by the combination of pyrimidine. Similarly, the geometry of BiBzIm comes from the literature.[17]

Results and Discussion

Preparations and Characterizations. The complex $[M(bpy)_2(BiBzImH_2)](ClO_4)_2$(M = Ru, Os) has a relatively weak acidic character; i.e. pK_{a1} = 5.74 and pK_{a2} = 10.51 for M = Ru, and pK_{a1} = 5.08 and pK_{a2} = 9.59 for M = Os.[12] The deprotonation of these complexes was accomplished in the presence of base to give the dideprotonated complex $[M(bpy)_2(BiBzIm)]^0$, which can act as a bidentate ligand. The complex $[M(bpy)_2(BiBzIm)]^0$ reacted with appropriate metal halides and bpy to form the dimeric complexes of general formula $[(bpy)_2M(BiBzIm)M'(bpy)_2]^{2+}$ (M = Ru, Os; M' = Ru, Os, Co, Ni). As the heterobinuclear metal complexes are liable to be contaminated by the homonuclear complexes, the purity was ensured each time by cyclic voltammetry and by measuring absorption spectra for different lots of preparative samples. For the preparation of $[(bpy)_2Ru(BiBzIm)Os(bpy)_2]^{2+}$, the reaction of $Ru(bpy)_2Cl_2$ with $Os(bpy)_2(BiBzIm)$ was utilized instead of the reaction of $Os(bpy)_2Cl_2$ with $Ru(bpy)_2(BiBzIm)$, because the substitution of Cl^- from $Os(bpy)_2Cl_2$ proceeds only under vigorous conditions.

The complexes $[(bpy)_2M(BiBzIm)M'(bpy)_2]^{2+}$ (M, M' = Ru, Os) are diamagnetic and have low-spin Ru(II) and Os(II) d^6 states. The complexes $[(bpy)_2Ru(BiBzIm)Co(bpy)_2]^{2+}$ and $[(bpy)_2Ru(BiBzIm)Ni(bpy)_2]^{2+}$ are both paramagnetic. The observed values of magnetic moments are respectively 4.92 and 3.24 μ_B for Ru-Co and Ru-Ni complexes, suggesting that high-spin octahedral Co^{2+} (d^7) and Ni^{2+} (d^8) ions are involved in these binuclear complexes.[18]

UV-Visible Spectra. The UV-visible absorption spectral data for complexes $[(bpy)_2M^{II}(BiBzIm)M'^{II}(bpy)_2]^{2+}$ are collected in Table I.

The absorption band at 510 nm corresponds to $d\pi-\pi^*$(bpy) metal-to-ligand charge-transfer (MLCT) transitions.[19] The intensity of the MLCT band for M' = Co(II) and Ni(II) is almost half of that for M' = Ru(II), which means that this band is attributable to the Ru $d\pi-\pi^*$(bpy) transition. The second $d\pi-\pi^*$(bpy) MLCT transition may be overlapped by the intense $\pi-\pi^*$(BiBzIm) intraligand bands. For the osmium binuclear complexes, additional absorption bands are observed at 670-740 nm, which can be assigned to a triplet $d\pi-\pi^*$ (bpy) MLCT transition.

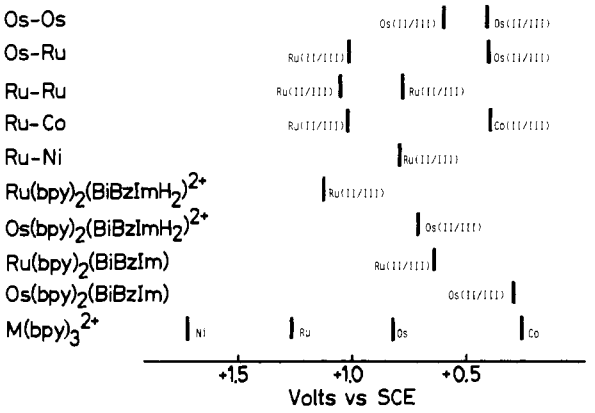

Figure 1. Oxidation potential diagram of $[(bpy)_2MBiBzIm)M(bpy)_2]^{2+}$ and related mononuclear complexes.

Electrochemistry for Oxidation Processes. Figure 1 shows the electrode oxidation potential of each binuclear BiBzIm complexes along with those of mononuclear $(bpy)_2M(BiBzIm)$ and $[M(bpy)_3]^{2+}$. More detailed electrochemical study on the present complexes will be reported in due course.[20]

For the homobinuclear Ru-Ru and Os-Os complexes, two successive electrode oxidation couples are observed. The separations in peak potentials, ΔE_p, are about 70 mV, and ratios of oxidation to reduction peak height are 1.0 ± 0.1, which indicates that the electrode oxidation processes are reversible. A one-electron process for each couple was also confirmed by coulometry.

The heterobinuclear Ru-Os and Ru-Co complexes also show two reversible couples. The first electrode oxidation process at a lower potential can be assigned as a Os(II/III) or Co(II/III) couple and the second oxidation process is assigned as a Ru(II/III) couple by comparison with the oxidation potential of the homonuclear complexes as well as those of $[M(bpy)_3]^{2+}$. The Ru-Ni complex shows only one reversible Ru(II/III) couple, while a Ni(II/III) couple has not been observed. It is found that the electrode oxidation potentials of two $M(bpy)_2$ sites are independent of each other.

If the oxidation potentials of binuclear complexes are compared with those of mononuclear ones, it is found that the first oxidation potentials of binuclear complexes are 0.3 V lower than those of the mononuclear complexes $[M(bpy)_2(BiBzImH_2)]^{2+}$. This indicates that the BiBzIm bridging ligand in binuclear complexes has an electron-donor property. On the contrary, the first oxidation potential of the binuclear $[(bpy)_2Ru(bpm)Ru(bpy)_2]^{4+}$ complex is 0.2 V higher than that of the mononuclear complex, in which bpm has been shown to act as an electron-acceptor ligand.

When the Ru(II/III) oxidation potential is regarded as a function of the metal ion in the second $M(bpy)_2$ site, the oxidation potential depends only on the charge of the second metal ion; i.e., the observed Ru(II/III) oxidation potentials are +0.78 and +1.0 V vs SCE for +2 and +3 charged second metal ions, respectively.

This result suggests that the electronic delocalization through BiBzIm is relatively small and the electrostatic interaction becomes

(15) Lexa, D.; Saveant, J. M.; Zickler, J. *J. Am. Chem. Soc.* **1977**, *99*, 2786.
(16) Binkley, J. S.; Whiteside, R. A.; Krishman, R.; Seeger, R.; Frees, D. J.; Schlegel, H. B.; Topiol, S.; Kahn, L. R.; Pople, J. A. *QCPE*, **1981**, *13*, 406.
(17) Uson, R.; Oro, L. A.; Gimeno, J.; Ciriano, M. A.; Cabeza, J. A.; Tiripicchio, A.; Camellini, M. T. *J. Chem. Soc., Dalton Trans.* **1983**, 323.
(18) The high-spin Co^{2+} and Ni^{2+} complexes generally have magnetic moments of 4.7-5.2 and 2.9-3.4 μ_B, respectively: Cotton, F. A.; Wilkinson, G. A. *Advanced Inorganic Chemistry*, 4th ed. Wiley: New York, 1980; pp 770, 786.
(19) (a) Felix, F.; Ferguson, J.; Gudel, H. J.; Ludi, A. *J. Am. Chem. Soc.* **1980**, *102*, 4096. (b) Decurtins, S.; Felix, F.; Ferguson, J.; Gudel, H. U.; Ludi, A. *J. Am. Chem. Soc.* **1980**, *102*, 4102. (c) Kober, E. M.; Meyer, T. J. *Inorg. Chem.* **1982**, *21*, 3967.
(20) Bond, A. M.; Haga, M., manuscript in preparation.

Table II. Oxidative Electrochemical Data for Binuclear and Mononuclear Complexes $[(bpy)_2M(BiBzIm)M'(bpy)_2](ClO_4)_2$ and $[M(bpy)_2(BiBzImH)_2](ClO_4)_2$ in CH_3CN (0.1 M TBAP) at a Platinum Electrode at 25 °C

M–M' or M	$E_{1/2}^r$, V vs SCE (ΔE_p, mV)[a]		
	Ru(II/III)	Os(II/III)	other
Ru–Ru	+0.77 (61), +1.06 (63)		
Ru–Os	+1.01 (64)	+0.39 (66)	
Ru–Co	+1.01 (62)		+0.37 (93) (Co(II/III))
Ru–Ni	+0.78 (62)		
Os–Os		+0.40 (68), +0.58 (65)	
Ru	+1.12 (70)		
Os		+0.66 (63)	

[a] The potentials $E_{1/2}^r$ are calculated from the equation $(E_{pa} + E_{pc})/2$ where E_{pa} and E_{pc} are respectively anodic and cathodic peak potentials. The values in parentheses are peak-to-peak separations, $\Delta E_p = E_{pc} - E_{pa}$.

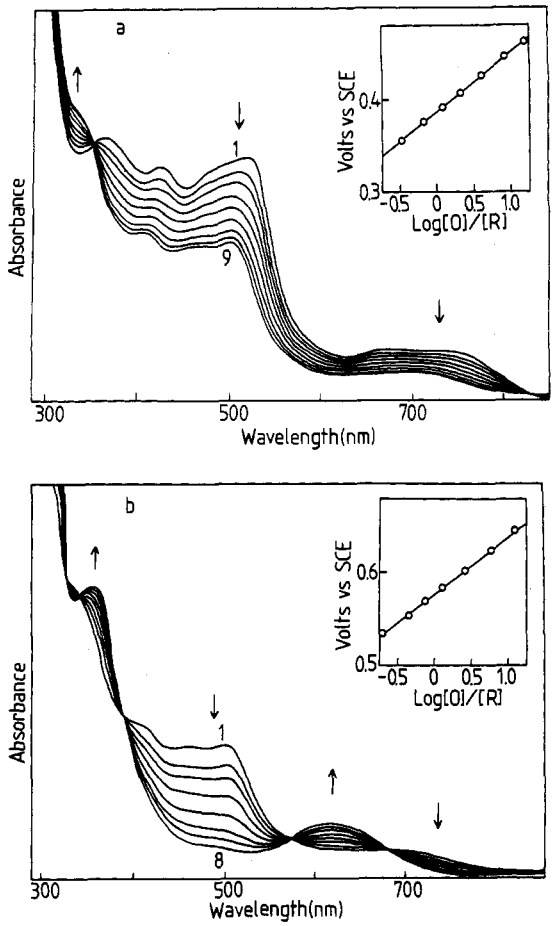

Figure 2. Spectroelectrochemistry of $[(bpy)_2Os(BiBzIm)Os(bpy)_2]^{2+}$ (9.8×10^{-4} M) in CH_3CN (0.1 M TBAP) at the following potentials (V vs SCE): (a) +0.20 (1), +0.34 (2), +0.36 (3), +0.38 (4), +0.39 (5), +0.41 (6), +0.43 (7), +0.45 (8), +0.46 (9); (b) + 0.53 (1), +0.55 (2), +0.57 (3), +0.58 (4), +0.60 (5), +0.62 (6), +0.64 (7), +0.80 (8). Nernst plots for a and b.

an important factor for determining the potential in the present system. The voltammetric data are summarized in Table II.

Spectroelectrochemical experiments on $[(bpy)_2Os(BiBzIm)Os(bpy)_2]^{2+}$, as shown in Figure 2, were performed by controlling the applied potentials. With increasing applied potential, the intensity of the absorption maxima of the Os(II)–Os(II) complex at 518 and 730 nm gradually decreases and isosbestic points are seen at 355 and 830 nm (Figure 2a). Nernst plots of applied potential E vs log ([Ox]/[Red]) in eq 1[21] yield $E^{\circ\prime} = +0.387$ V

$$E = E^{\circ\prime} + (0.059/n) \log ([Ox]/[Red]) \quad (1)$$

vs SCE and $n = 1.0$, which are in good agreement with the voltammetric result. Electrolysis at more positive applied potential causes the complete loss of MLCT band at 505 nm and the appearance of a new band at 618 nm with four isosbestic points at 341, 386, 571, and 680 nm. This new band can be assigned as a bpy → Os(III) ligand-to-metal charge-transfer (LMCT) transition. Nernst plots at 505 nm give $E^{\circ\prime} = +0.577$ V vs SCE for the Os(II)–Os(III)/Os(III)–Os(III) couple and $n = 1.01$. Similarly the absorption spectra of $[(bpy)_2Ru(BiBzIm)Ru(bpy)_2]^{n+}$ during stepwise one-electron exhausive oxidation exhibit a significant decrease of the MLCT band at 505 nm. A blue shift of the MLCT band after one-electron oxidation is also observed.

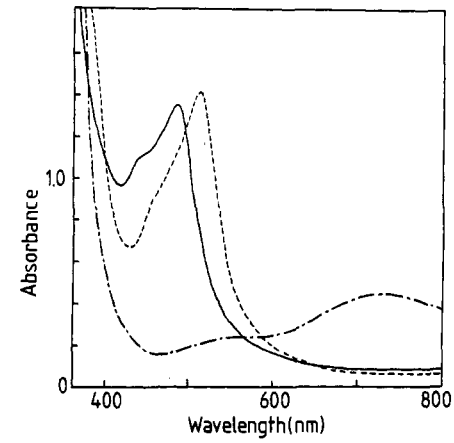

Figure 3. Visible absorption spectra of $[(bpy)_2Ru(BiBzIm)Co(bpy)_2]^{n+}$ (7.5×10^{-4} M) on the electrochemical oxidation in CH_3CN (0.1 M TBAP): before electrolysis ($n = 2$, --), after electrolysis at +0.5 V ($n = 3$, —), and after electrolysis at +1.2 V vs SCE ($n = 4$, -·-).

Figure 3 shows the UV–visible spectra at potentials corresponding to the three accessible oxidation states of $[(bpy)_2Ru(BiBzIm)Co(bpy)_2]^{2+}$. When the Ru(II)–Co(II) complex is oxidized at +0.5 V vs SCE, the MLCT absorption maximum at 512 nm is shifted to shorter wavelengths ($\lambda_{max} = 485$ nm). This blue shift on the MLCT absorption band during the first oxidation of Co(II) to the Co(III) state suggests an acceptor property of Co(III) greater than that of Co(II). Further oxidation at +1.2 V vs SCE to the Ru(III)–Co(III) state drastically changes the MLCT absorption; i.e., the absorption maximum at 485 nm disappeared, and a new peak at 730 nm appeared.

Spectroelectrochemical oxidation of $[(bpy)_2Ru(BiBzIm)Ni(bpy)_2]^{2+}$ at +1.0 V vs SCE leads to the complete loss of the MLCT absorption band at 513 nm and the appearance of a new band with low intensity at 758 nm.

Exhaustive electrooxidation of $[(bpy)_2Ru(BiBzIm)Os(bpy)_2]^{2+}$ at +0.7 V vs SCE leads to a significant decrease of the MLCT band at 482 nm and a complete loss of the triplet MLCT band attributed to Os(II) complex. After the second oxidation at +1.2 V vs SCE, a complete loss of the MLCT band and an appearance of new weak band at 604 nm is observed. As mentioned before, the first and second oxidation processes are respectively Os(II/III) and Ru(II/III) oxidations.

In summary, the blue shift of MLCT band was found after the first metal M' oxidation because of the greater electron accepting ability of M'(III) than that of M'(II), and the second oxidation leads to the complete loss of the MLCT band for the complexes

(21) Heineman, W. R. *J. Chem. Educ.* **1983**, *60*, 305.

Table III. Comparison of Oxidation Potentials and Comproportionation Values K_{com} for the Binuclear Complexes with Different Bridging Ligand L at 25 °C

	$Ru(bpy)_2$–			$Os(bpy)_2$–		
L	$E_{1/2}$, V vs SCE	$\Delta E_{1/2}$,[a] V	K_{com},[b] M^{-1} cm^{-1}	$E_{1/2}$, V vs SCE	$\Delta E_{1/2}$,[a] V	K_{com},[b] M^{-1} cm^{-1}
BiBzIm	+0.77 +1.06	0.29	8.2×10^4	+0.40 +0.58	0.18	1.1×10^3
pz[c]	+0.83 +1.21	0.38	2.8×10^6			
bpm[d]	+1.53 +1.69	0.16	5.2×10^2			

[a] Potential difference between $E_{1/2}$ values. [b] Calculated from the equation $\Delta E_{1/2} = 0.0591 \log K_{com}$. [c] pz = pyrazolate.[40] [d] Reference 7b.

Table IV. Near-Infrared Spectral Data for $[(bpy)_2M(BiBzIm)M'(bpy)_2]^{n+}$ in CH_3CN[a]

		ν_{max}, cm^{-1} (ϵ, M^{-1} cm^{-1})			
		IT transition		$d\pi$–$d\pi$ transition	
M–M′	n				
Os(II)–Os(III)	3	8180 (1800)	4800 (500)[b]	5450 (960)	4400 (300)
Ru(II)–Os(III)	3	9570 (1430)	5580 (810)	5110 (620)	<4000[c]
Ru(II)–Ru(III)	3	9420 (1300)	5130 (3400)		
Os(III)–Os(III)	4			5340 (1060)	4310 (700)
Ru(III)–Os(III)	4			5300 (510)	4290 (380)

[a] The mononuclear complex $[Os(bpy)_2(BiBzImH_2)]^{3+}$ shows near-infrared bands at 5290 (ϵ = 330) and 4270 cm^{-1} (ϵ = 270). [b] This band is obtained after subtraction of $d\pi$–$d\pi$ bands from the observed band at 4810 cm^{-1}. [c] Only the tail of the band is observed because of the detection limit of spectrophotometer.

$[(bpy)_2M(BiBzIm)M'(bpy)_2]^{n+}$ (M = Ru, Os; M′ = Ru, Os, Co, Ni).

The comproportionation equilibrium constant K_{com} (see eq 2) can be calculated from eq 3 by using the potential difference

$$[M^{II}\text{–BiBzIm–}M^{II}]^{2+} + [M^{III}\text{–BiBzIm–}M^{III}]^{4+} \xrightleftharpoons{K_{com}} 2[M^{II}\text{–BiBzIm–}M^{III}]^{3+} \quad (2)$$

$$\Delta E_{1/2} = 0.0591 \log K_{com} \quad \text{(at 25 °C)} \quad (3)$$

between two couples, $\Delta E_{1/2}$ ($=E_2 - E_1$). The calculated comproportionation constants are collected in Table III.

It is worth noting that the K_{com} value of the Os complex is much smaller than that of the Ru complex. In the Ru and Os mixed-valence complexes previously studied, the K_{com} values of the Os complexes are much larger than those of Ru complexes.[3a,22] For example, the K_{com} value of $[[Os(NH_3)_5]_2(pyz)]^{6+}$ (pyz = pyrazine) has been reported as 7×10^{12}, which is 10^7-fold greater than that of the diruthenium analogue ($K_{com}(Ru) = 4 \times 10^6$).[22] Similarly, the K_{com} values of $[[(bpy)_2ClM]_2(pyz)]^{2+}$ are 1600 for M = Os and 100 for M = Ru.[23]

IT Bands in the Near-Infrared Region. The binuclear complexes $[(bpy)_2M(BiBzIm)M'(bpy)_2]^{n+}$ (M, M′ = Os, Ru) exhibit rich near-infrared spectra, while no near-infrared spectra are observed for $[(bpy)_2Ru(BiBzIm)M'(bpy)_2]^{n+}$ (M′ = Co, Ni; n = 2–4) (Table IV).

Figure 4 shows the near-infrared absorption spectra of $[(bpy)_2Os(BiBzIm)Os(bpy)_2]^{n+}$ (n = 2–4). The starting Os(II)–Os(II) complex (n = 2) shows the tail of a triplet $Os(d\pi) \rightarrow bpy(\pi^*)$ transition above 11 000 cm^{-1}, but is otherwise transparent in the near-infrared region. The fully oxidized Os(III)–Os(III) complex (n = 4) shows two narrow bands at 4310 and 5340 cm^{-1}. Similar near-infrared bands at 4270 and 5290 cm^{-1} are also observed in the monomeric $[Os(bpy)_2(BiBzImH_2)]^{3+}$ complex;[24] however, the bands are almost half of the intensity of the fully oxidized binuclear complex (n = 4). These two near-infrared transitions can be assigned as $d\pi$–$d\pi$ transitions by comparison

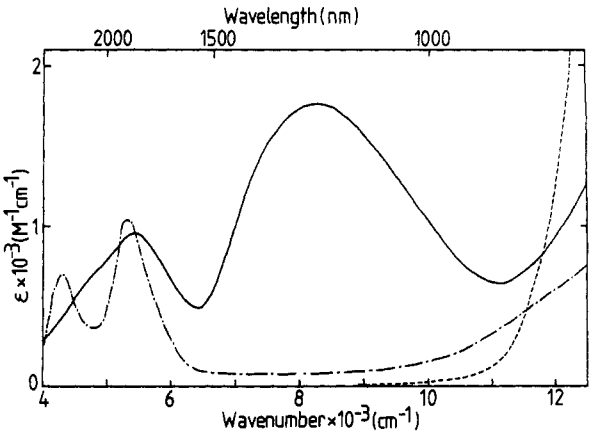

Figure 4. Near-infrared spectra of $[(bpy)_2Os(BiBzIm)Os(bpy)_2]^{n+}$ (3.8×10^{-3} M) on the electrochemical oxidation in CH_3CN (0.1 M TBAP): before electrolysis (n = 2, - -), at +0.5 V (n = 3, —), and at +1.0 V vs SCE (n = 4, –·–).

with the near-infrared spectra of other monomeric and binuclear Os(III) complexes reported previously.[25]

The mixed-valence Os(II)–Os(III) complex (n = 3) exhibits two broad bands at 5450 and 8180 cm^{-1}. Even for mixed-valence complexes, the $d\pi$–$d\pi$ transitions localized at the Os(III) site are expected to occur at the same energy with half of the intensity of those for the fully oxidized Os(III)–Os(III) complex. After subtraction of $d\pi$–$d\pi$ bands from the lower energy band, the spectrum still reveals the presence of the band at 4800 cm^{-1}. Thus, the two bands at 4800 and 8180 cm^{-1} can be attributed to different electronic components of the intervalence-transfer (IT) transition:

$$[(bpy)_2Os^{II}(BiBzIm)Os^{III}(bpy)_2]^{3+} \xrightarrow{h\nu} [(bpy)_2Os^{III}(BiBzIm)Os^{II}(bpy)_2]^{3+*} \quad (4)$$

Several mixed-valence Ru and Os complexes have been reported to exhibit multiple IT bands.[26] Multiple IT bands of particular

(22) Magnuson, R. H.; Lay, P. A.; Taube, H. *J. Am. Chem. Soc.* **1983**, *105*, 2507.
(23) (a) Callahan, R. W.; Keene, F. R.; Meyer, T. J.; Salmon, D. J. *J. Am. Chem. Soc.* **1977**, *99*, 1064. (b) Kober, E. M. Ph.D. Thesis, University of North Carolina, 1982.
(24) In symmetries lower than O_h, the six-fold degenerate $^2T_{2g}$ ground state of $(d\pi)^5$ configuration is resolved into three Kramers doublets (E_1', E_2', E_3') and their orbital splitting can be described by the effective spin–orbit coupling constant λ and tetragonal parameter Δ.[27] Assuming C_2 symmetry for $[(Os(bpy)_2(BiBzImH_2)]^{3+}$, the values of λ = 3013 cm^{-1} and Δ = 1790 cm^{-1} are obtained.
(25) (a) Sen, J.; Taube, H. *Acta Chem. Scand. Ser. A* **1979**, *33*, 125. (b) Buhr, J. D.; Winkler, J. R.; Taube, H. *Inorg. Chem.* **1980**, *19*, 2416.
(26) (a) Joss, S.; Reust, H.; Ludi, A. *J. Am. Chem. Soc.* **1981**, *103*, 981. (b) Magnuson, R. H.; Taube, H. *J. Am. Chem. Soc.* **1972**, *94*, 7213. (c) Richardson, D. E.; Sen, J. P.; Buhr, J. D.; Taube, H. *Inorg. Chem.* **1982**, *21*, 3136. (d) Joss, S.; Burgi, H. B.; Ludi, A. *Inorg. Chem.* **1985**, *24*, 949. (e) Dubicki, L.; Ferguson, J.; Krausz, E. R.; Lay, P. A.; Maeder, M.; Magnuson, R. H.; Taube, H. *J. Am. Chem. Soc.* **1985**, *107*, 2167. (f) Kober, E. M.; Goldsby, K. A.; Narayana, D. N. S.; Meyer, T. J. *J. Am. Chem. Soc.* **1983**, *105*, 4303.

Table V. Properties of the Intervalence-Transfer Bands for $[(bpy)_2M(BiBzIm)M'(bpy)_2]^{3+}$ and $[(bpy)_2M(bpm)M'(bpy)_2]^{5+}$

			obsd[b]			calcd[c]	
M–M'	L	d,[a] Å	$\bar{\nu}_{max}$, cm^{-1}	ϵ_{max}, M^{-1} c^{-1}	$\Delta\nu_{1/2}$, cm^{-1}	$\Delta\bar{\nu}_{1/2}$(calcd), cm^{-1}	α^2
Ru–Ru	BiBzIm	5.5	5130	3300	2300	3440	2.0×10^{-2}
Ru–Ru	bpm	5.6	5000[d]			3400	
Ru–Os	BiBzIm	5.5	9570	1430	3520	3300	7.3×10^{-3}
Ru–Os	bpm	5.6	8080[d]	330	4400	3400	2.4×10^{-3}
Os–Os	BiBzIm	5.5	8180	1800	3370	4350	1.0×10^{-2}

[a] The distance between sites. [b] In CH_3CN. [c] Calculated by using eq 7 and 8 in the text. [d] Reference 7b.

systems such as $[(bpy)_2OsCl(PPh_2CH_2PPh_2)OsCl(bpy)_2]^{3+}$ have been analyzed semiquantitatively in consideration of the three IT transitions separated by the energy difference between spin–orbit states at the Os(III) site in mixed-valence complexes.[26f] The simple relationships between the IT transition energy, E_{IT}, and the energy between spin–orbit states, E_{SO}, have been derived; i.e.

$$\Delta E_1 = E_{IT,2} - E_{IT,1} = E_{SO,1} \quad (5)$$

$$\Delta E_2 = E_{IT,3} - E_{IT,1} = E_{SO,2} \quad (6)$$

The same spectral analysis has been applied to the present binuclear system. As the first $d\pi$–$d\pi$ transition occurs at 4310 cm^{-1} for the present Os(III)–Os(III) complex, the band at 4800 cm^{-1} can be assigned to the first IT band corresponding to the transition Os(II), A_1-Os(III), 1E′ → Os(III), 1E′-Os(II), A_1. The band at 8180 cm^{-1} can be assigned to the second IT transition Os(II), A_1-Os(III), 1E′ → Os(III), 2E′-Os(II), A_1. The energy difference between the first and second IT transitions, $\Delta E_1 \approx 3400$ cm^{-1}, is in fair agreement with the energy of the first spin–orbit band, $E_{SO,1} = 4300$ cm^{-1}. The third IT band would occur at 10 100 cm^{-1}, however this band would be overlapped by the tail of the second IT band and not be resolvable.

The near-infrared absorption spectra of $[(bpy)_2Os(BiBzIm)Ru(bpy)_2]^{n+}$ (n = 2, 3, 4) are shown in Figure 5. The Os(II)–Ru(II) complex exhibits only the tail of a triplet Os($d\pi$) → bpy(π^*) and/or Ru($d\pi$) → bpy(π^*) transition above 10000 cm^{-1} in the near-infrared region. The fully oxidized Os(III)–Ru(III) complex shows two $d\pi$–$d\pi$ absorption bands at 4290 and 5300 cm^{-1} and the large tail above 7000 cm^{-1} due mainly to bpy(π) → Ru($d\pi$) transition, and partially to bpy(π) → Os($d\pi$). The mixed-valence Os(III)–Ru(II) complex exhibits four near-infrared absorption bands at 5110, 5580, and 9570 cm^{-1} with the tail of the fourth band below 4000 cm^{-1} (the limit of detection). The lower two bands at 4000 cm^{-1} and 5110 cm^{-1} can be assigned to the $d\pi$–$d\pi$ transitions, 1E′ → 2E′ and 1E′ → 3E′, which are localized at the Os(III) site compared to those of the analogous Os complex.[25] Two other bands at 5580 and 9570 cm^{-1} could be assigned to the IT transitions. The energy difference between two IT transitions is ~4000 cm^{-1}, which should correspond to the energy between spin–orbit states of Ru(III).

Preliminary results have been reported on the multiple IT bands at 5130 and 9420 cm^{-1} for the mixed-valence $[(bpy)_2Ru(BiBzIm)Ru(bpy)_2]^{3+}$ complex.[8] An energy difference between two IT bands of $\Delta E \approx 4300$ cm^{-1} is observed, which is comparable with the value for $[(bpy)_2Os(BiBzIm)Ru(bpy)_2]^{3+}$ ($\Delta E \approx 4000$ cm^{-1}). This agreement can be attributed to about the same splitting of the energy levels at the optically prepared Ru(III) site in both complexes. A tetragonal distortion and spin–orbit coupling split the $^2T_{2g}$ state arising from the t_{2g}^5 configuration into three Kramers doublets,[27] since the present Ru–Ru and Os–Ru binuclear complexes have C_2 symmetry. Consequently, the energy difference within one of the Kramers doublets is predicted to be ~4000 cm^{-1}. For the present system, the absorption bands corresponding to the predicted energy difference within the Ru(III) states have not been observed so far; however, the transition within the Kramers doublets has been reported in several Ru(III) complexes. The observed transitions are 3950 cm^{-1} for *mer*-$RuCl_3(PBu_3Ph)_3$[27a]

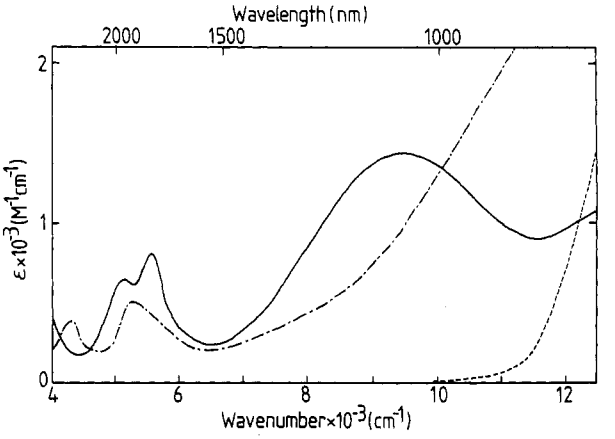

Figure 5. Near-infrared spectra of $[(bpy)_2Os(BiBzIm)Ru(bpy)_2]^{n+}$ in CH_3CN (0.1 M TBAP): n = 2 (- -), 3 (—), 4 (- · -).

and 6700 cm^{-1} for Ru(meR)$_3$ (meR = *N*-methylthiohydroxamate).[28] More sophisticated MO treatments and techniques supporting the spectral analysis are required to understand the multiple IT bands in the present system.

The bandwidths at half-intensity, $\Delta\nu_{1/2}$ (cm^{-1}), for well-defined IT bands, obtained by doubling the low-energy side, are collected in Table V, along with the values for bpm-bridged Ru and Os complexes.[7b]

A lower limit for bandwidth at room temperature, $\Delta\bar{\nu}_{1/2}$(calcd), can be calculated from the equation given by Hush[29]

$$\Delta\bar{\nu}_{1/2}(\text{calcd}) = [2.31 \times 10^3(\bar{\nu}_{max} - \Delta E)]^{1/2} \quad (\text{in } cm^{-1}) \quad (7)$$

where $\bar{\nu}_{max}$ is the wavenumber of the IT absorption maximum and ΔE is the internal energy difference between the sites. The observed bandwidths are narrower than those calculated except that for $[(bpy)_2Os(BiBzIm)Ru(bpy)_2]^{3+}$. The comparison between observed and calculated values of bandwidth has been used to assess the extent of delocalization;[3] for the valence-localized complexes, $\Delta\bar{\nu}_{1/2}$(obsd) is generally larger than $\Delta\bar{\nu}_{1/2}$(calcd). Furthermore, the extent of delocalization α^2 can also be estimated from the properties of the IT bands by using the Hush equation[29]

$$\alpha^2 = 4.24 \times 10^{-4}\epsilon_{max}\Delta\nu_{1/2}/(d^2\bar{\nu}_{max}) \quad (8)$$

where ϵ_{max} is the extinction coefficient (in M^{-1} cm^{-1}), and d is the distance between sites (in Å). For the BiBzIm bridging system, the value d = 5.5 Å can be used on the basis of X-ray crystal structures of analogous $[Rh_2(COD)_2(BiIm)]$ (COD = 1,5-cyclooctadiene and BiIm = 2,2′-biimidazolate)[30] and $[Cu_2(Me_5dien)_2(BiIm)](BPh_4)_2$ (Me_5dien = 1,1,4,7,7-pentamethyldiethylenetriamine).[31] The calculated α^2 values are shown in Table V. The α^2 values obtained were 7.3×10^{-3} to 2.0×10^{-2}. These values are relatively larger than those of other mixed-valence

(27) (a) Hudson, A.; Kennedy, M. J. *J. Chem. Soc. A* **1969**, 1116. (b) Hill, N. J. *J. Chem. Soc., Faraday Trans. 2.* **1979**, *68*, 427. (c) Kober, E. M.; Meyer, T. J. *Inorg. Chem.* **1983**, *22*, 1614.

(28) Bhattacharya, S.; Ghosh, P.; Chakravorty, A. *Inorg. Chem.* **1985**, *24*, 3224.

(29) (a) Hush, N. S. *Trans. Faraday Soc.* **1961**, *57*, 557. (b) Hush, N. S. *Prog. Inorg. Chem.* **1967**, *8*, 391. (c) Hush, N. S. *Electrochim. Acta* **1968**, *13*, 1005.

(30) Kaiser, S. W.; Saillant, R. B.; Butler, W. M.; Rasmussen, P. G. *Inorg. Chem.* **1976**, *15*, 2681.

(31) Haddad, M. S.; Duesler, E. N.; Hendrickson, D. N. *Inorg. Chem.* **1979**, *18*, 141.

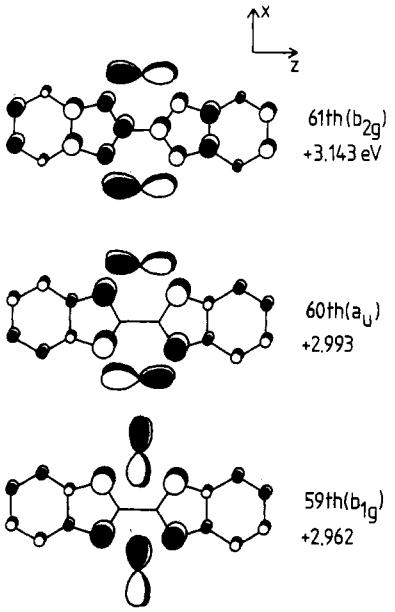

Figure 6. Proposed scheme of three Lπ–dπ[M(III)] orbital mixings. The numbers denote MO energy level numbers of $BiBzIm^{2-}$, where the 61st MO is the HOMO (totally, 61 × 2 electrons).

complexes such as $[[(bpy)_2(ClRu]_2(pyz)]^{2+}$;[3a,23a] however, the values still fall within Robin and Day's class II for mixed-valence complexes.[32]

Characteristics of BiBzIm and bpm as Bridging Ligands. Both $[(bpy)_2Ru(bpm)Ru(bpy)_2]^{3+}$ and $[(bpy)_2Ru(BiBzIm)Ru(bpy)_2]^{3+}$ exhibit IT absorption bands at almost same wavenumbers, 5000 cm^{-1}. However, the stability for the two complexes is quite different; while $[(bpy)_2Ru(bpm)Ru(bpy)_2]^{5+}$ is not stable on a preparative time scale,[7b] $[(bpy)_2Ru(BiBzIm)Ru(bpy)_2]^{3+}$ is stable. In order to shed light on this stability difference, the electronic structures of bridging ligands $BiBzIm^{2-}$ and bpm have been investigated by using ab initio molecular orbital calculations with the STO-3G basis set.[33] The electronic density on the nitrogen atom of BiBzIm (7.38) is appreciably larger than that of bpm (7.23), which indicates that $BiBzIm^{2-}$ is a stronger σ donor. The 56th and 57th occupied orbitals of $BiBzIm^{2-}$ (E = 0.944 and 1.190 eV) are in-plane π orbitals, which can contribute to σ-type bonding interactions between $BiBzIm^{2-}$ and metal ions. The 58th to 61st out-of-plane π orbitals (E = 1.265 and 3.143 eV) are much higher than the corresponding levels of bpm (−8.954 and −8.649 eV). Among four, three out-of-plane π orbitals (59th, 60th, and 61st) of $BiBzIm^{2-}$ can lead to stronger π donation from $BiBzIm^{2-}$ to vacant dπ levels on M(III) ions as shown in Figure 6. Thus, the strong σ-donor property of BiBzIm and greater M(III)dπ–$BiBzIm^{2-}(\pi)$ mixing result in more sufficient dissociative stability of BiBzIm-bridged mixed-valence complexes. In addition, the dianionic BiBzIm ligand reduces the cationic charge of Ru and Os metals on the mixed-valence complex and also decreases the electrostatic repulsion between the two positive charged metal centers.

The stability of $[(bpy)_2M(BiBzIm)M'(bpy)_3]^{3+}$ (M = Ru, Os) is ascribed to the attainment of the aromaticity of BiBzIm. The neutral BiBzIm is unstable, and its dianion is stable in the sense that it has 20π electrons like "two naphthalenes". The negatively charged ligand has a small ionization potential and has the ability to donate the electronic charge well to the cationic metal in the π direction. Such charge transfer and the Coulombic attraction between two counterions (negative ligand and positive metal) are not effective in $[(bpy)_2Ru(bpm)Ru(bpy)_2]^{5+}$.

The present Ru complex has a larger comproportionation constant K_{com} compared to that of the analogous Os complex. This is contrary to the results for other Ru and Os complexes reported so far.[3a,34] This anomaly can be also accounted for by the extent of orbital mixing. First, energy levels of out-of-plane π orbitals of BiBzIm are closer to those of vacant dπ levels of Ru than to those of Os, which will lead to greater mixing between BiBzImπ and dπ(M(III)) orbitals for Ru. Second, the extent of the overlap between bridging BiBzIm and metal orbitals is expected to depend on the metal–nitrogen distance and the "bite" angle of the bridging BiBzIm. The relation between molecular structures and the magnetic coupling for imidazolate-bridged copper binuclear complexes has been extensively discussed.[35] Unfortunately, the molecular structures of the present Ru and Os binuclear complexes are not known, but the structures of analogous BiBzIm- and BiIm-bridged (BiIm = 2,2′-biimidazolate) complexes have already been determined. The bite angles of $[Cu_2(Me_5dien)_2(BiIm)]^{2+}$,[31] $Rh_2(COD)_2(BiIm)$,[30] and $NEt_4[Ir(COD)(PPh_3)(Tcbiim)]\cdot CH_2Cl_2$ (Tcbiim = tetracyanobiimidazolate)[36] are 82.78, 82.5, and 75.3°, respectively. The smaller bite angles predominantly result from their larger metal–nitrogen bond lengths. As the third-row Os–N bond is a little longer than the second-row Ru–N one,[37] the "bite" angle of BiBzIm would be too small for the Os complex to give an efficient overlap between nitrogen lone pairs and Os d orbitals. In addition, the magnitude of the antisymmetric MO overlap (60th and 61st—d_{yz}) shown in Figure 6 is sensitive to the size of d orbitals and is larger in the Ru complex than in the Os complex.

The presence of the higher lying occupied out-of-plane π orbitals in BiBzIm leads to the effective Lπ–dπ(M(III)) orbital interaction, resulting in a higher stability against the dissociation of the BiBzIm-bridged mixed-valence complexes relative to that of the bpm-bridged ones. A similar Lπ–dπ interaction has been so far reported only in the $[(Ru(NH_3)_5)_2(L\text{-}L)]^{4+}$ system (L-L = deprotonated *tert*-butylmalononitrile).[3a,38]

In conclusion, the characteristics of the present BiBzIm-bridged Os and Ru binuclear complexes are summarized.

1. These complexes belong to the Robin and Day's class II.
2. Multiple IT absorption bands are observed, which comes from the orbital splitting of optically prepared M(III) site by tetragonal distortion and spin–orbit coupling.
3. K_{com} for the Ru(II)–Ru(III) commplex is found to be larger than that of the Os(II)–Os(III) complex.
4. The higher stability shown in these complexes than in analogous bpm binuclear complexes is attributable to the superior donor property of the anionic $BiBzIm^{2-}$ ligand.

Registry No. $[(bpy)_2Ru(BiBzIm)Ru(bpy)_2](ClO_4)_2$, 90364-24-2; $[(bpy)_2Ru(BiBzIm)Os(bpy)_2](ClO_4)_2$, 110904-51-3; $[(bpy)_2Ru(BiBzIm)Co(bpy)_2](ClO_4)_2$, 110904-53-5; $[(bpy)_2Ru(BiBzIm)Ni(bpy)_2](ClO_4)_2$, 110904-55-7; $[(bpy)_2Os(BiBzIm)Os(bpy)_2](ClO_4)_2$, 110904-57-9; $[(bpy)_2Os(BiBzIm)Os(bpy)_2]^{3+}$, 110934-46-8; $[(bpy)_2Ru(BiBzIm)Os(bpy)_2]^{3+}$, 110904-58-0; $[(bpy)_2Ru(BiBzIm)Ru(bpy)_2]^{3+}$, 90364-25-3; $[(bpy)_2Os(BiBzIm)Os(bpy)_2]^{4+}$, 110904-59-1; $[(bpy)_2Ru(BiBzIm)Os(bpy)_2]^{4+}$, 110904-60-4; $Os(bpy)_2(BiBzIm)$, 104642-31-1; $[Os(bpy)_2(BiBzImH_2)](ClO_4)_2$, 104642-28-6; $Os(bpy)_2Cl_2$, 15702-72-4; $Ru(bpy)_2Cl_2$, 15746-57-3; $Ru(bpy)_2(BiBzIm)$, 88437-60-9; $BiBzImH_2$, 6965-02-2.

(32) (a) Robin, M. B.; Day, P. *Adv. Inorg. Chem. Radiochem.* **1967**, *10*, 247. (b) Day, P. In *Mixed-Valence Compounds*; Brown, D., Ed.; D. Reidel: Dordrecht, The Netherlands, 1980; p 3.
(33) The bpm molecule is found to be slightly nonplanar with the twisting angle with the two ring planes at 12.6°. In contrast, $BiBzIm^{2-}$ is calculated to be planar.
(34) (a) Rillema, D. P.; Callahan, R. W.; Mack, K. B. *Inorg. Chem.* **1982**, *21*, 2589. (b) Rillema, D. P.; Mack, K. B. *Inorg. Chem.* **1982**, *21*, 3849. (c) Rillema, D. P.; Allen, G.; Meyer, T. J.; Conrad, D. *Inorg. Chem.* **1983**, *22*, 1617.
(35) (a) Haddad, M.; Hendrickson, D. N. *Inorg. Chem.* **1978**, *17*, 2622. (b) Bencini, A.; Benelli, C.; Gatteschi, D.; Zanchini, C. *Inorg. Chem.* **1986**, *25*, 398 and references cited therein.
(36) Rasmussen, P. G.; Bailey, O. H.; Bayon, J. C.; Butler, W. M. *Inorg. Chem.* **1984**, *23*, 343.
(37) Hambley, T. W.; Lay, P. A. *Inorg. Chem.* **1986**, *25*, 4553.
(38) Krentzien, H.; Taube, H. *J. Am. Chem. Soc.* **1976**, *98*, 6379.
(39) Russel, G. A.; Konaka, R. *J. Org. Chem.* **1967**, *32*, 234.
(40) Sullivan, B. P.; Salmon, D. J.; Meyer, T. J.; Peedin, J. *Inorg. Chem.* **1979**, *18*, 3369.